

# Microstructures and friction–wear performances of cathodic arc ion plated TiAlN coatings on YT14 cemented carbide cutting tools

Kong Dejun<sup>a)</sup>

*School of Mechanical Engineering, Changzhou University, Changzhou 213164, People's Republic of China; and Jiangsu Key Laboratory of Materials Surface Science and Technology, Changzhou University, Changzhou 213164, People's Republic of China*

Zhang Donghui and Guo Haoyuan

*School of Mechanical Engineering, Changzhou University, Changzhou 213164, People's Republic of China*

(Received 9 November 2016; accepted 22 February 2017)

A TiAlN coating was deposited on a YT14 cemented carbide cutting tool using a cathodic arc ion plating, the surface–interface morphologies, chemical elements, phases, and microhardness of the obtained TiAlN coating were analyzed with a field emission scanning electronic microscope, energy dispersive spectrometer, X-ray diffraction, and microhardness tester, respectively, and the coating surface roughness and grain scale were characterized with a atomic force microscope. The bonding strength of the coating was measured with a scratch tester, and the friction–wear properties were investigated with a reciprocation type friction–wear tester. The results show that the bonding strength of the coating is 54.9 N, and the coating microhardness reaches 2724 HV. The average coefficient of friction of the coating is 0.59, the wear mechanism is abrasive wear and slight brittle fracture.

## I. INTRODUCTION

The transition-metal nitride coating of TiN has previously been applied in the surface modification of cutting tools to increase wear performance and service life<sup>1</sup> because of its high hardness and high abrasion resistance. However, the working temperature of oxidation resistance is only 550 °C,<sup>2</sup> which can hardly meet the cutting requirements of hard machining materials.<sup>3</sup> For further improving the wear performance of TiN coating, Al atoms are added into the TiN coating to form TiAlN coating, which improves the hardness and wear resistance. The mechanical and tribological performances of TiN coating have been increased,<sup>4</sup> which satisfy the ever-growing demands of modern industrial applications.<sup>5</sup> TiAlN coating can be deposited using a chemical vapor deposition (CVD), cathode arc ion plating (CAIP), and reactive magnetron sputtering (RMP),<sup>6</sup> among them, the CAIP is widely used as a hard coating deposition technique because it has many advantages such as high deposition rate and strong bonding strength between the coating and the substrate.<sup>7</sup> The TiAlN coating on cutting tools is demonstrated to have excellent high-temperature stability,<sup>8</sup> mechanical properties,<sup>9</sup> and wear resistance,<sup>10</sup> which has been attracted many attentions in China and abroad. The addition of Al atoms into the FCC (face centered cubic) structure of TiN coating forms a TiAlN

coating, the grain refinement of the TiAlN coating improves its hardness, high temperature oxidation, and wear resistance.<sup>11</sup> The presence of Al in the TiAlN coating overcomes the oxidation problems due to a superficial layer of Al<sub>2</sub>O<sub>3</sub> formed at high temperature, which restricts oxygen diffusion and oxidative wear.<sup>12</sup> The researches focus on mainly studying the deposition methods, growth mechanisms, and mechanical performances of the TiAlN coating.<sup>13</sup> At present, the research works had been done on cutting performance and service life of the TiAlN coating on cutting tools.<sup>14</sup> To date, the energy spectrum analysis and wear mechanism of the TiAlN coating have been rarely investigated. In this study, a TiAlN coating was deposited on YT14 cemented carbide cutting tools with a CAIP, the surface–interface morphologies, distributions of chemical elements, phases, and microhardness were analyzed with a field emission scanning electronic microscope (FESEM), energy dispersive spectrometer (EDS), X-ray diffraction (XRD), and microhardness tester, respectively, and bonding strength of the coating interface was characterized with a scratch tester. In addition, the friction–wear characteristics of the coating were investigated by using a multifunctional material surface tester which provided an experimental basis for evaluating the surface application in cutting tools.

## II. EXPERIMENTAL

The experimental substrate was commercial YT14 cemented carbide cutting tools, which composed of TiC, WC, and Co as a binder; the chemical compositions were shown as follows (wt%): WC 78, TiC 14, Co 8.

Contributing Editor: Jürgen Eckert

<sup>a)</sup>Address all correspondence to this author.

e-mail: kong-dejun@163.com

DOI: 10.1557/jmr.2017.86

Before being deposited, the samples were ground by the sandpapers of 80#–1200#, metallographic sandpaper, and polishing on a P-2T type polishing machine in turn (Guangzhou Weiyi Metallographic Test Instrument Co., Ltd., Guangzhou, China). Moreover, the samples were cleaned in pure acetone using ultrasonic oscillation, rinsed in pure ethanol, and dried up before being deposited in a PVT (plasmaund vakuum technik gmbh) coating system. The working gas was Ar with a high purity of 99.99%, and reaction gas was N<sub>2</sub> with a high purity of 99.99%, the target was a Ti–Al alloy target with an atom fraction rate of 1:1.

Before being deposited, the alloy target was etched with ions for 30 min to remove the organic adhesion complexes and oxidation layer of the target surface. The deposition parameters are shown in Table I. The surface–interface morphologies and chemical compositions of the obtained TiAlN coating were analyzed with a JSUPRA55 type FESEM (Carl Zeiss AG, Oberkochen, Germany), and its configured EDS, respectively, the phases of the coating were analyzed with a 2500PC type XRD (Rigaku Corporation, Tokyo, Japan), and the coating topography and grain scales were analyzed with a

TABLE I. Deposition parameters of TiAlN coating.

Items	Bias voltage/V	Target arc currents/A	Duty cycles/%	Partial pressure of N/Pa	Temperature/°C	Time/min
Parameters	–100	60	30	$8 \times 10^{-3}$	400	120

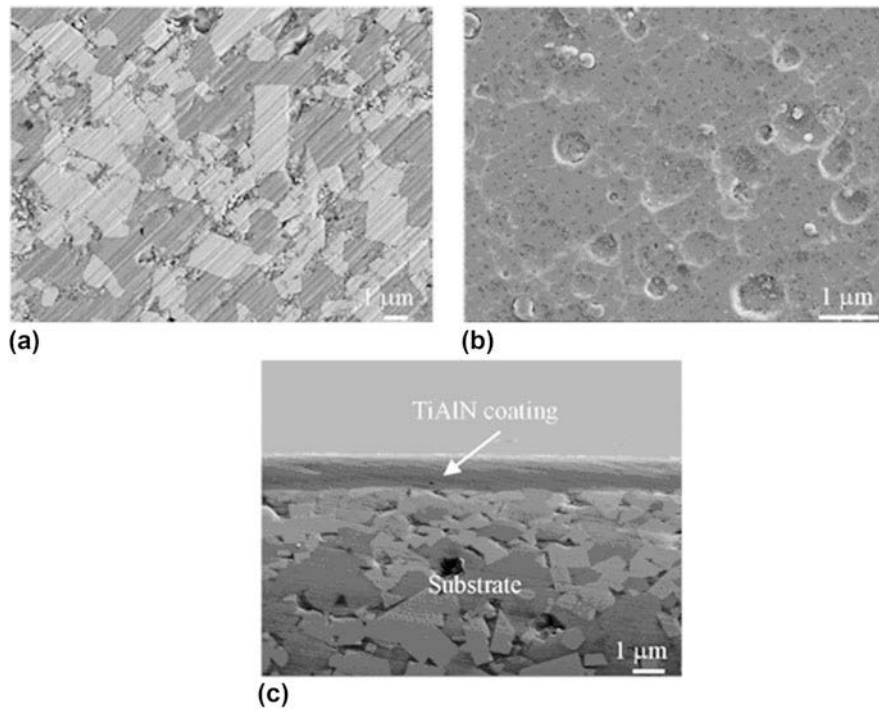


FIG. 1. Morphologies of a YTi4 cemented carbide cutting tool surface and TiAlN coating surface–interface: (a) substrate morphology; (b) coating surface morphology; (c) coating interface morphology.

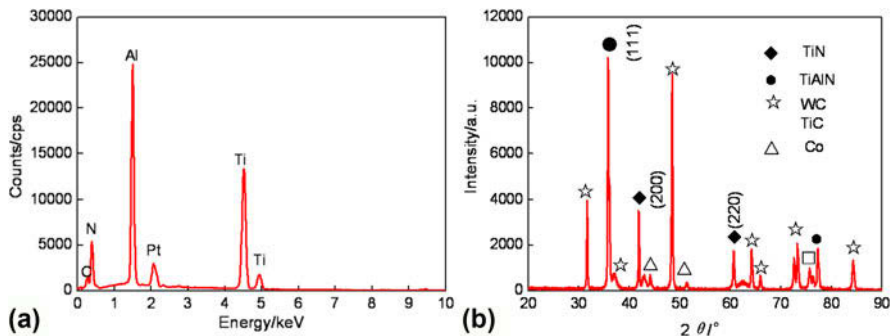


FIG. 2. EDS and XRD analysis of TiAlN coating: (a) EDS analysis; (b) XRD analysis.

CSPM5500 type atomic force microscope (AFM; Original Nano-Instrument Co. Ltd., Beijing, China). The bonding strength of the coating interface was measured with a WS-2005 type film scratch tester (Lanzhou Zhongkai Science and Technology Development Co. Ltd., Lanzhou, China), the measurement method was acoustic emission, test parameters: load of 100 N, loading rate of 50 N/min, and scratch length of 4 mm. The microhardness of the coating was measured with a HV-1000 type micro-Vivtorinox hardness tester (Guangzhou Weiyi Metallographic Test Instrument Co. Ltd., Guangzhou, China), test parameters: load of 0.2 N, time of 15 s, the coating microhardness was presented with the average value in five times measurement. The friction and wear performances of the coating were investigated with a CFT type multifunctional material surface tester (Lanzhou Zhongkai Science and Technology Development Co. Ltd., Lanzhou, China), test parameters: load of 5 N, test time of 30 min, friction mode: sliding, friction pair: ceramic ball ( $\text{Si}_3\text{N}_4$ ) with a diameter of 4 mm, running speed of 500 times/min, and running length of 3 mm.

### III. ANALYSIS AND DISCUSSION OF RESULTS

#### A. Surface–interface morphologies

Figure 1(a) shows the surface morphology of a YT14 cemented carbide cutting tool after grinding. The visible WC and TIC particles were distributed in the binder Co, which remained the high hardness for the substrate. The surface roughness was  $\sim 0.1 \mu\text{m}$  measured with a TR240 type surface roughness tester (Beijing Times Technology Co. Ltd., Beijing, China).

The obtained TiAlN coating was continuously and uniformly distributed, as shown in Fig. 1(b). There was

no particle spallation, this was because CAIP was accompanied by the emission of particles when the plasma was produced with high energy at the high density state. The coating thickness was  $\sim 1.5 \mu\text{m}$ , as shown in Fig. 1(c), the coating structures at the bonding interface were compact and were closely combined with the substrate.

#### B. EDS and XRD analysis

The EDS analysis result of TiAlN coating is shown in Fig. 2(a), and the mass fractions and atomic fractions are shown in Table II. The TiAlN coating was primarily composed of Ti, Al, and N, in addition, the appeared C element came from the contaminated products in the air. The mass fraction ratio of Ti/Al in the coating was close to 2:1, compared with the Ti and Al elements in the alloy targets, the mass fraction ratio of Ti and Al was 1:1, which was increased. The low Al content improved lattice distortion structure defects in the coatings and caused the lattice distortion for a constant lattice increase, which decreased the coating roughness<sup>15</sup> and changed the crystal preferred orientation of the coating growth,<sup>16</sup> this was due to the difference of resputtering rate of Ti and Al atoms.

The phase result of the TiAlN coating was measured by an XRD analysis with a  $\text{Cu K}\alpha_1$  radiation ( $\lambda = 1.54056 \text{ \AA}$ ), as shown in Fig. 2(b), the diffraction peaks of TiAlN (ICDD card no. 71-5864) at the diffraction angle of  $37^\circ$  and TiN (ICDD card no. 06-0642)<sup>17</sup> at the diffraction angles of  $44^\circ$  and  $63^\circ$  were detected, respectively. For the TiN phase, the TiN energies of crystal planes (200) and (220) were minimized, therefore, the preferential growth of TiN was along crystal planes (200) and (220), and the microstructure of the coating was the TiN phase. When the Al was added to the TiN to replace the part of Ti, the diffraction peak shifted to a low angle, the spacing of crystal planes became large. The TiAlN coating was preferred to grow in the crystal plane (111), the lattice structure was still FCC structure.<sup>13</sup> Because the thickness of the TiAlN coating was very thin, the substrate peaks of WC (ICDD card no. 51-0939), TiC (ICDD card no 32–1383), and Co (ICDD card no 15-0806)<sup>17</sup> were detected by X-ray.

TABLE II. EDS analysis result of TiAlN coating.

Elements	Ti	Al	N	C
Mass fraction (wt%)	30.93	16.19	43.62	9.26
Atomic fraction (at%)	12.58	11.69	60.69	15.03

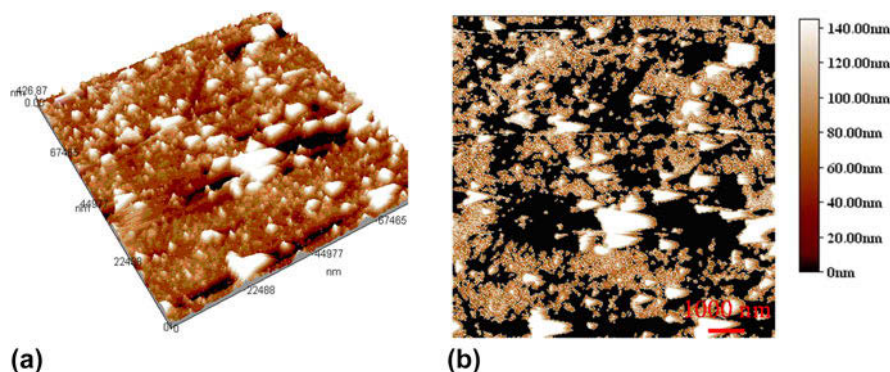


FIG. 3. AFM topography and particle distribution of TiAlN coating surface: (a) AFM topography; (b) particle distribution.

### C. AFM analysis

Figure 3 shows the AFM topography and grain scale of the TiAlN coating using the AFM configured imager 4.60 software, the corresponding amplitude and gain scale parameters are shown in Table III. The amplitude parameters were small, as shown in Fig. 3(a), the coating surface fluctuated a little, showing that the surface quality of the TiAlN coating had a well friction performance. The grain scales on the TiAlN coating with a smooth process are shown in Fig. 3(b), the total grain number of the TiAlN coating was 2691, the corresponding average area, diameter, and height was  $1.69 \times 10^6 \text{ nm}^2$ , 463.9 nm, and 14.62 nm, respectively. According to the Hall–Petch equation,<sup>14</sup> the smaller the particle size was, the higher the material hardness was. As a result, the TiAlN coating had high microhardness due to fined grains, which was 2724 HV measured by five times on a HV-1000 micro-Vivtorinox hardness tester. Compared with

TABLE III. Roughness parameters and grain size parameters of TiAlN coating.

Amplitude parameters	Grain scale parameters		
Average roughness of $S_a/\text{nm}$	8.2	Total number of particles	2691
Mean square root of $S_q/\text{nm}$	11.7	Average area/ $\text{nm}^2$	$1.69 \times 10^6$
Surface skewness of $S_{sk}$	1.14	Average diameter/nm	463.90
Surface kurtosis of $S_{ku}$	10.4	Average height/nm	14.62
Peak–peak of $S_p/\text{nm}$	145	Maximum height/nm	74.04
Ten point height of $S_z/\text{nm}$	144	Minimum height/nm	1.16

2150 HV of TiN coating,<sup>18</sup> the microhardness of TiAlN coating was increased by about 27%. This was because that the addition of Al in the coating formed TiAlN coating with the low content of Al, which not only had an effect of solid solution hardening but also changed the coating microstructure and crystallographic orientation.

### D. Energy spectrum analysis of surface and interface

The chemical element distributions of the coating in Fig. 1(b) were analyzed with a plane scan analysis, Ti, Al, N, and C were detected, among them, C was the contaminated products on the TiAlN coating in the air. There were black spots existed on the plane energy spectrum of Ti, Al, and N elements, which was because that the ions bombarded the coating surface, the resputtering effect caused the pores during the deposition, resulting in uneven local distribution of Ti, Al, and N elements, as shown in Fig. 4(a)–4(c).

Figure 5(a) shows the line scanned position of the coating interface. Ti, Al, and N of the coating interface presented a gradient distribution; the contents of chemical elements in the coating were gradually reduced, as shown in Figs. 5(b)–5(d). Ti, Al, and N were diffused at the interface, which improved the bonding state between the coating and the substrate. This was because that at the initial stage of deposition, the coating was covered on the substrate. The C content in the substrate was high, as

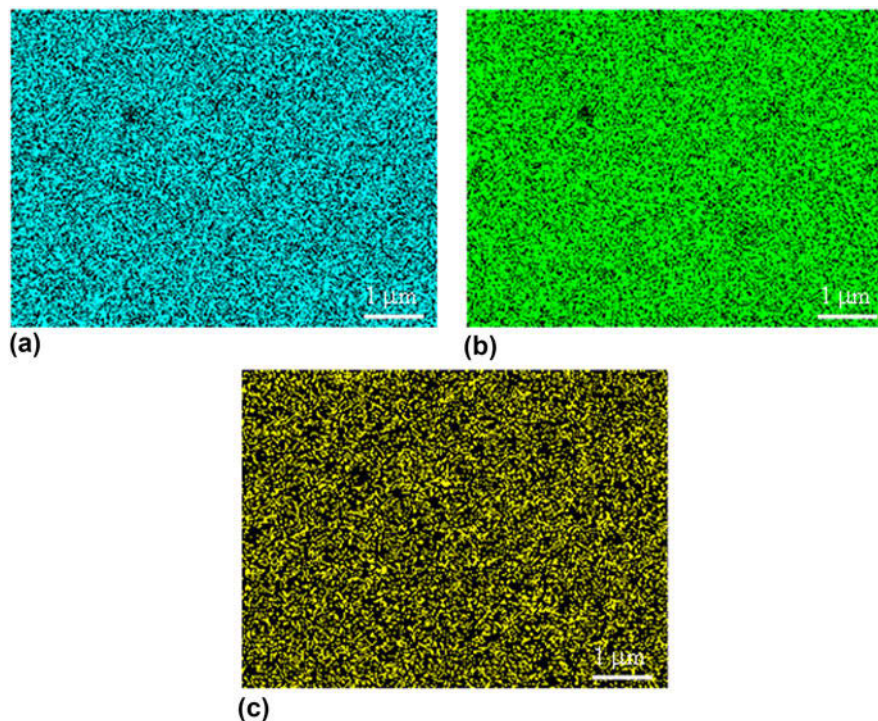


FIG. 4. Plane scans of TiAlN coating surface: (a) Ti content; (b) Al content; (c) N content.

shown in Fig. 5(e), this was because that the hard carbide cutting tool was primarily composed of WC and TiC.<sup>19</sup> W and Co in the substrate did not produce a diffusion phenomenon, as shown in Figs. 5(f)–5(g).

Figure 6(a) shows the position of the plane scan analysis at the coating interface, the result of the plane scan analysis is shown in Fig. 6(b), and the corresponding data are shown in Table IV. Ti, Al, and N formed a gradient diffusion layer at the interface, and there was a small amount of elements penetrating into the substrate, as shown in Figs. 6(c)–6(e). The boundary of the coating–substrate interface was obvious, and there was a stratification phenomenon, which was mechanical combination. The C distribution is shown in Fig. 6(f), coming from the substrate. As shown in Figs. 6(g)–6(h), the W and Co elements were distributed in the substrate, there was no diffusion. Therefore, the interface of the TiAlN coating was mechanical bonding, accompanied with local metallurgical bonding.

## E. Interface bonding strength

The diamond head with a radius of 0.2 mm was used to scratch on the TiAlN coating surface, when the load gradually increased to a certain value, there was break-off phenomenon that appeared between the coating and the substrate,<sup>20</sup> as shown in Fig. 7(a). At the point, the critical load was the bonding strength of the coating interface, showing that the binding strength of the TiAlN coating was 54.9 N, as shown in Fig. 7(b).

## F. Friction and wear performance

Figure 8(a) shows the relationship between COFs and wear time, the average COF was 0.59, of which the uncertainty was decided by the coating surface roughness and measurement errors.<sup>21</sup> In the running-in period (0–10 min), the COF was increased rapidly with large fluctuation. This was because that the particles and pits of the coating surface made the friction resistance increase sharply, and the average

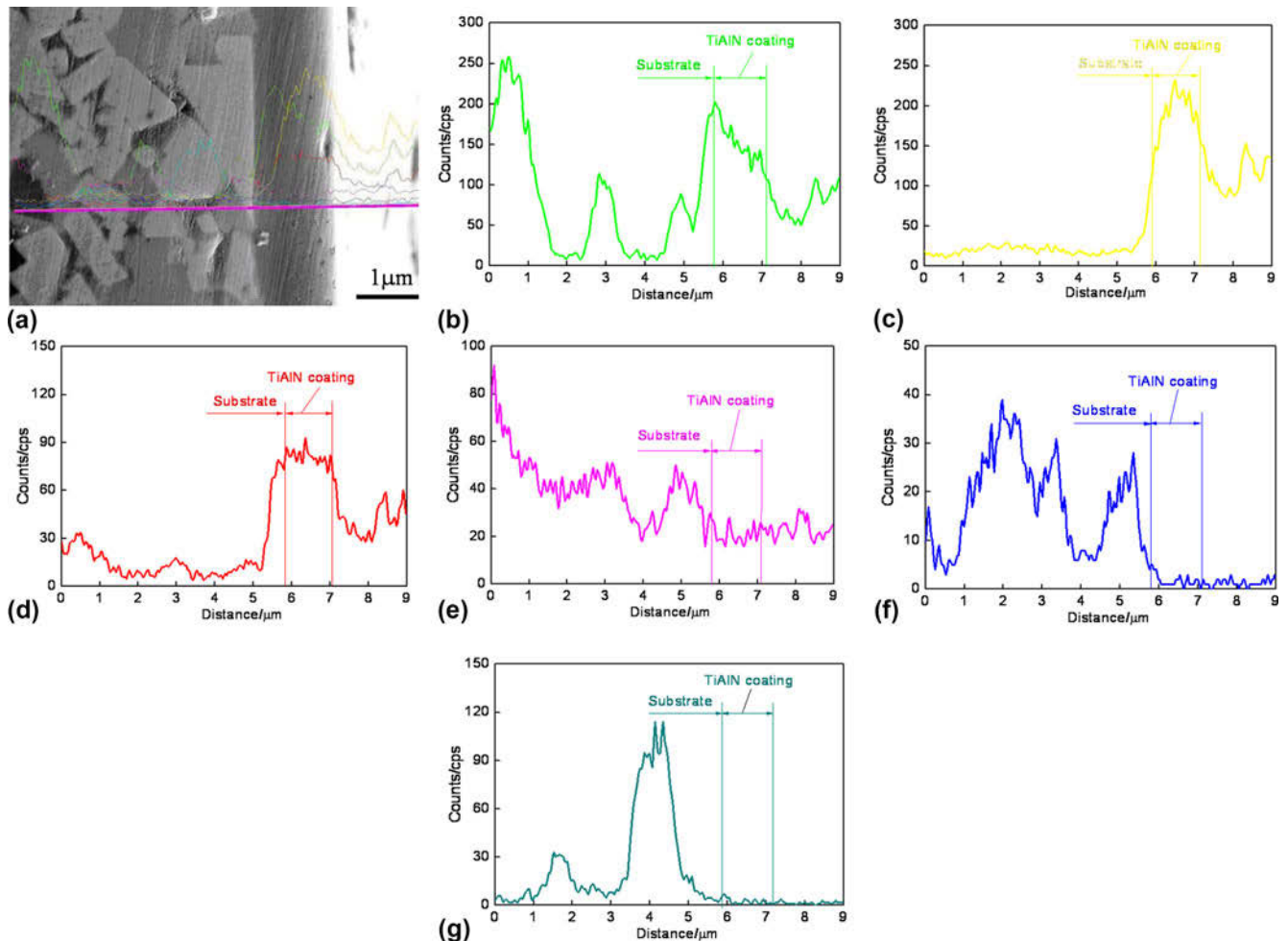


FIG. 5. Line scan analysis of TiAlN coating interface: (a) line scanned position; (b) Ti content; (c) Al content; (d) N content; (e) C content; (f) W content; (g) Co content.

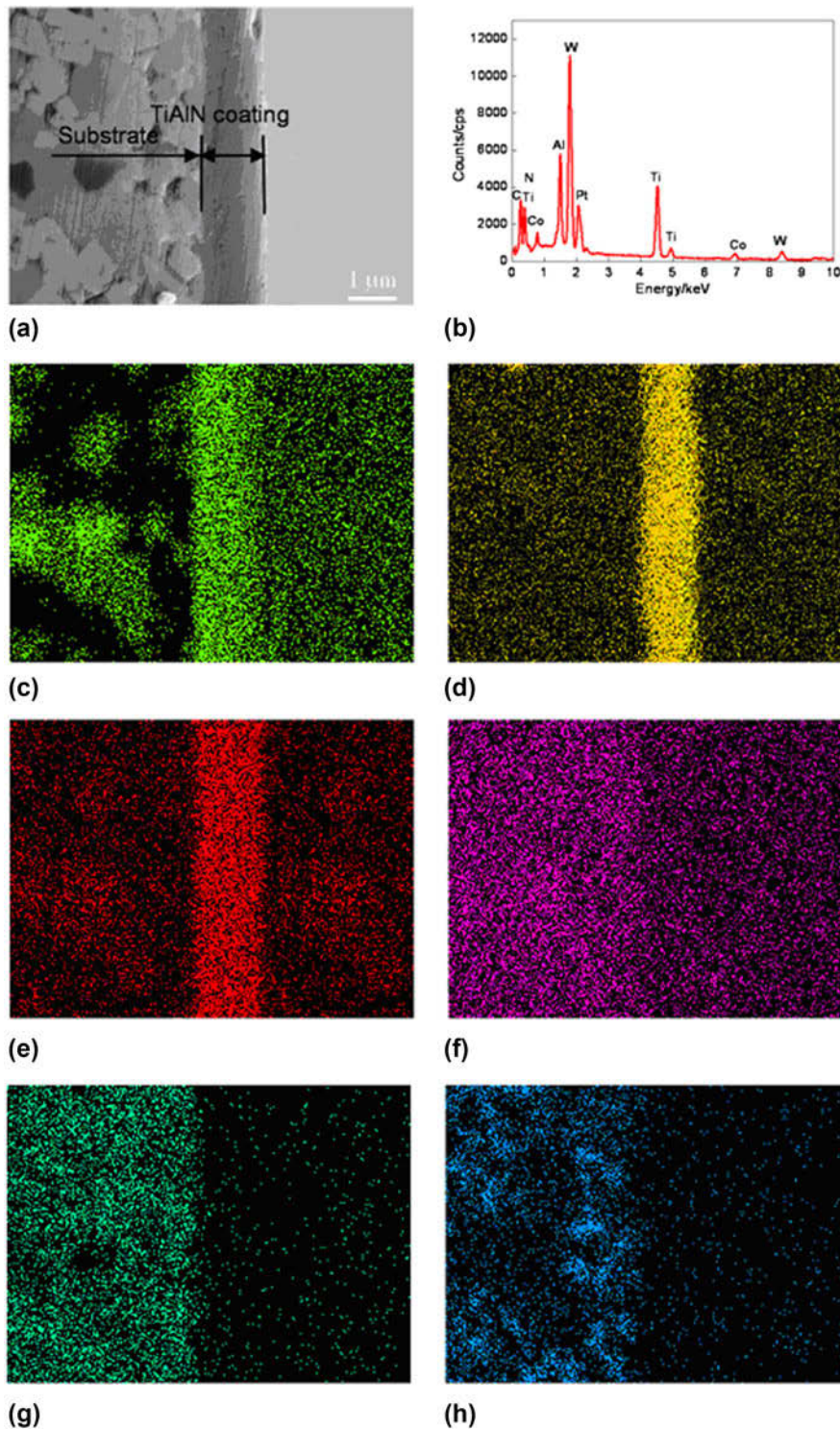


FIG. 6. Plane scans of TiAlN coating interface: (a) plane scanned position; (b) result of plane scan analysis; (c) Ti content; (d) Al content; (e) N content; (f) C content; (g) W content; (h) Co content.

COF was 0.56. The COF was gradually reduced with the wear time increasing. This was because the surface of the TiAlN coating was constantly polished. At the stable period (10–30 min), the average COF was 0.44, the TiAlN coating had high wear resistance.<sup>22</sup> The

TABLE IV. Plane scan analysis result of TiAlN coating interface.

Elements	Ti	Al	N	C	W	Co
Mass fraction (wt%)	10.74	3.62	35.80	22.32	25.32	2.19
Atomic fraction (at%)	4.53	2.71	51.66	37.56	2.78	0.75

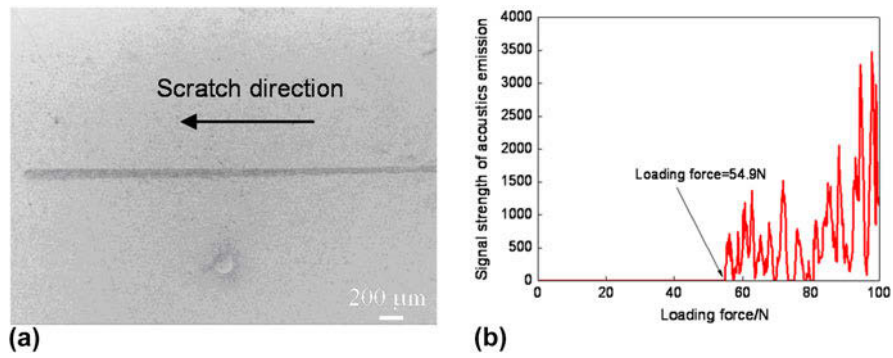


FIG. 7. Scratch morphology and bonding strength of TiAlN coating: (a) scratch morphology; (b) binding strength.

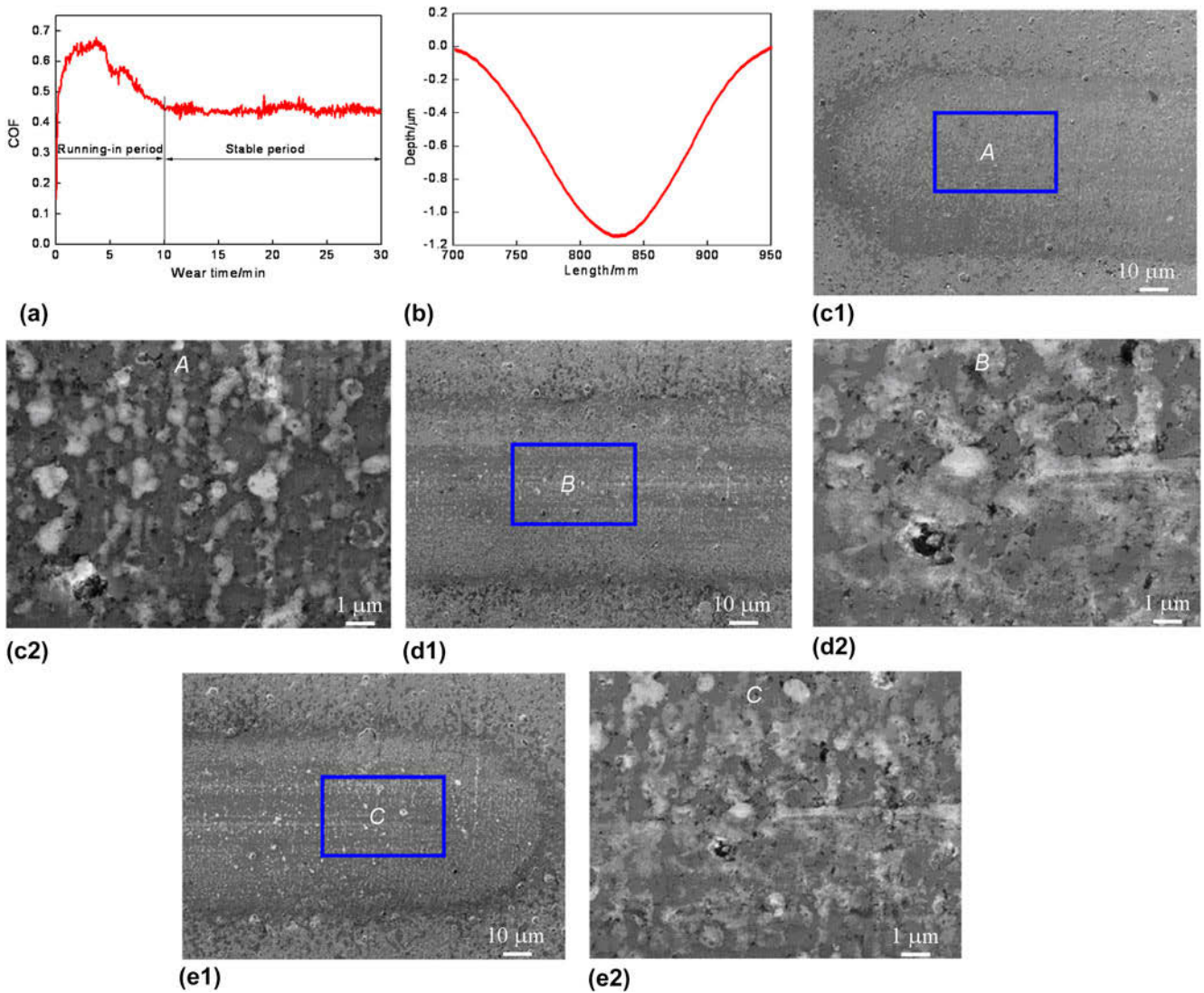


FIG. 8. COFs and wear profile of TiAlN coating: (a) COFs versus wear time; (b) wear profile; (c) initiating zone; (d) central zone; (e) ended zone.

wear volume of the TiAlN coating is shown in Fig. 8(b), the selected surface baseline was  $-1.335 \mu\text{m}$ , the width and depth of wear profile were

$318 \mu\text{m}$ ,  $2.335 \mu\text{m}$ , respectively, and the wear rate was  $1.73 \times 10^{-5} \text{ mm}^3/\text{N m}$ , which indicated that the coating had high wear resistance.

After the wear test, the TiAlN coating surface was covered with a layer of debris, the number of wear debris at the initiating and terminal ends was the most, there were some obvious thin furrows, as shown in Fig. 8(c). This was due to the friction effect of wear debris on the coating, there were some obvious wear phenomena. In the wear process, the cracks occurred, which caused larger wear debris. It verified that large particles of the coating surface occurred brittle fracture under the action of reciprocating friction,<sup>23</sup> as shown in Fig. 8(d). In the course of friction, the wear debris at the worn scar edges were continuously removed, so the chip removal capacity was strong.<sup>24</sup> As shown in Fig. 8(e), the wear mechanism of the TiAlN coating was abrasive wear, accompanied by slight brittle fracture.

#### IV. CONCLUSIONS

(1) The TiAlN coating with a microhardness of 2724 HV is composed of TiN and TiAlN phases.

(2) Ti, Al, and N are combined with mechanical bonding at the interface, accompanied with locally metallurgical bonding, the interface bonding strength is 54.9 N.

(3) The average COF of TiAlN coating is 0.59, and the wear mechanism is abrasive wear + slight brittle fracture, showing deducing friction and wear resistance.

#### ACKNOWLEDGMENTS

Financial support for this research by the Jiangsu Province Science and Technology Support Program (Industry) (BE2014818) is gratefully acknowledged.

#### REFERENCES

- F. Vaz, P. Machado, L. Rebouta, P. Cerqueira, Ph. Goudeau, J.P. Riviere, E. Alvesc, K. Pischowd, and J. de Rijkd: Mechanical characterization of reactively magnetron-sputtered TiN films. *Surf. Coat. Technol.* **174–175**, 375 (2003).
- R.L. Niu, J.L. Li, Y.X. Wang, J.M. Chen, and Q.J. Xue: Structure and high temperature tribological behavior of TiAlN/nitride duplex treated coatings on Ti6Al4V. *Surf. Coat. Technol.* **309**, 232 (2017).
- A. Thakur and S. Gangopadhyay: Dry machining of nickel-based super alloy as a sustainable alternative using TiN/TiAlN coated tool. *J. Cleaner Prod.* **129**, 256 (2016).
- A. AL-Bukhaiti, K.A. Al-hatab, W. Tillmann, F. Hoffmann, and T. Sprute: Tribological and mechanical properties of Ti/TiAlN/TiAlCN nanoscalemultilayer PVD coatings deposited on AISI H11 hot work tool steel. *Appl. Surf. Sci.* **318**, 180 (2014).
- C.J. Feng, S.L. Hu, Y.F. Jiang, N.M. Wu, M.S. Li, L. Xin, S.L. Zhu, and F.H. Wang: Effects of Si content on microstructure and mechanical properties of TiAlN/Si<sub>3</sub>N<sub>4</sub>-Cu nanocomposite coatings. *Appl. Surf. Sci.* **320**, 689 (2014).
- D.K. Li, J.F. Chen, C.W. Zou, J.H. Ma, P.F. Li, and Y. Li: Effects of Al concentrations on the microstructure and mechanical properties of Ti–Al–N films deposited by RF-ICPIS enhanced magnetron sputtering. *J. Alloys Compd.* **609**, 239 (2014).
- S.H. Chang, Y.K. Lin, and K.T. Huang: Study on the thermal erosion, wear and corrosion behaviors of TiAlN/oxy-nitriding duplex-treated AISI H13 alloy steel. *Surf. Coat. Technol.* **207**, 571 (2012).
- R. Wang, J.L. Li, Y.X. Wang, J.M. Hu, and H.Z. Wu: High temperature oxidation behavior and mechanical properties of TiAlN/SiN decorative films on borosilicate glass by magnetron sputtering. *Thin Solid Films* **584**, 72 (2015).
- C.W. Zou, J. Zhang, W. Xie, L.X. Shao, and D.J. Fu: Structure and mechanical properties of Ti–Al–N coatings deposited by combined cathodic arc middle frequency magnetron sputtering. *J. Alloys Compd.* **509**, 1989 (2011).
- B.J. Liu, B. Deng, and Y. Tao: Influence of niobium ion implantation on the microstructure, mechanical and tribological properties of TiAlN/CrN nano-multilayer coatings. *Surf. Coat. Technol.* **240**, 405 (2014).
- M. Keunecke, C. Stein, K. Bewilogua, W. Koelker, D. Kassel, and H. van den Berg: Modified TiAlN coatings prepared by d.c. pulsed magnetron sputtering. *Surf. Coat. Technol.* **205**, 1273 (2010).
- Ł. Tomaszewski, W. Gulbinski, A. Urbanowicz, T. Suszko, A. Lewandowski, and W. Gulbinski: TiAlN based wear resistant coatings modified by molybdenum addition. *Vacuum* **121**, 223 (2015).
- D.J. Kong and G.Z. Fu: Nanoindentation analysis of TiN, TiAlN and TiAlSiN coatings prepared by cathode ion plating. *Sci. China: Technol. Sci.* **58**(1), 1360 (2015).
- Y. Long, J.J. Zeng, D.H. Yu, and S.H. Wu: Microstructure of TiAlN and CrAlN coatings and cutting performance of coated silicon nitride inserts in cast iron turning. *Ceram. Int.* **40**, 9889 (2014).
- C.W. Zou, J. Zhang, W. Xie, L.X. Shao, L.P. Guo, and D.J. Fu: Characterization and properties of Ti–Al–Si–N nano-composite coatings prepared by middle frequency magnetron sputtering. *Appl. Surf. Sci.* **257**, 10373 (2011).
- L. Escobar-Alarcón, D.A. Solís-Casados, S. Romero, M. Fernández, J. Pérez-Álvarez, and E. Haro-Poniatowski: Effect of aluminum plasma parameters on the physical properties of Ti–Al–N thin films deposited by reactive crossed beam pulsed laser deposition. *Appl. Surf. Sci.* **283**, 808 (2013).
- A.A. Matei, I. Pencea, M. Branzei, D.E. Trancă, G. Țepeș, C.E. Sfăt, E. Ciovea (Coman), A.I. Gherghilescu, and G.A. Stanciu: Corrosion resistance appraisal of TiN, TiCN and TiAlN coatings deposited by CAE-PVD method on WC–Co cutting tools exposed to artificial sea water. *Appl. Surf. Sci.* **358**, 572 (2015).
- F. Quesada, A. Mariño, and E. Restrepo: TiAlN coatings deposited by magnetron sputtering on previously treated ASTM A36 steel. *Surf. Coat. Technol.* **201**, 2925 (2006).
- M. Kalinn and J. Jerina: The effect of temperature and sliding distance on coated (CrN, TiAlN) and uncoated nitrided hot-work tool steels against an aluminium alloy. *Wear* **330–331**, 371 (2015).
- B.J. Liu, B. Deng, and Y. Tao: Influence of niobium ion implantation on the microstructure, mechanical and tribological properties of TiAlN/CrN nano-multilayer coatings. *Surf. Coat. Technol.* **240**, 405 (2014).
- D.J. Kong and H.Y. Guo: Analysis of structures and bonding strength of AlTiN coatings by cathodic ion plating. *Appl. Phys. A: Mater. Sci. Process.* **119**, 309 (2015).
- A.H. Liu, J.X. Deng, H.B. Cui, Y.Y. Chen, and J. Zhao: Friction and wear properties of TiN, TiAlN, AlTiN and CrAlN PVD nitride coatings. *Int. J. Refract. Met. Hard Mater.* **31**, 82 (2012).
- R. Ramadoss, N. Kumar, R. Pandian, S. Dash, T.R. Ravindran, D. Arivuoli, and A.K. Tyagi: Tribological properties and deformation mechanism of TiAlN coating sliding with various counterbodies. *Tribol. Int.* **66**, 143 (2013).
- S. Sveen, J.M. Andersson, R.M. Saoubi, and M. Olsson: Scratch adhesion characteristics of PVD TiAlN deposited on high speed steel, cemented carbide and PCBN substrates. *Wear* **308**(1–2), 133 (2013).